nature communications

Article

https://doi.org/10.1038/s41467-025-58633-5

Synthesis of benzoheterocycles by palladium-catalyzed migratory cyclization through an unexpected reaction cascade

Received: 8 July 2024

Accepted: 25 March 2025

Published online: 09 April 2025

Check for updates

Wen-Cong Li[1,2,3,4], Lin Zhang[2], Shiming Bai[4], Jia-Hao Zhao[1,3], Guang-Rui Liu[1,3], Yu Lan[2,5] ✉, Shufeng Chen[1] ✉ & Jialin Ming[1,3] ✉

Migratory functionalization of C−H bonds through metal migration from carbon to carbon under transition metal catalysis is a process of significant academic and industrial interest. Herein, a palladium-catalyzed migratory cyclization of α-bromoalkene derivatives ArXCBr=CH_2, in which X denotes a phosphorus (P(O)R), silicon (SiR_2), sulfur (SO_2), carbon (C(O)), nitrogen (NTs), or oxygen-based moiety, affording various benzoheterocyclic compounds has been developed. Mechanistic investigations have demonstrated that the cyclization reaction proceeds through an unexpected cascade, with *trans*-1,2-palladium migration between sp^2 carbons being a key step of catalytic cycle. To the best of our knowledge, this type of metal migration has not been reported previously.

Migratory functionalization of C−H bonds through metal migration from carbon to carbon under transition metal catalysis is a process of significant academic and industrial interest[1–12]. It provides a non-classical means of selectively installing a functional group at a remote C−H position using simple precursors, thus enabling the direct synthesis of challenging structures not accessible through traditional cross-couplings. Most notably, migratory functionalization of alkenes or alkyl halides through a 1,2-metal shift along a sp^3 chain and cross-coupling has been well developed for remote C−H bond functionalization (Fig. 1)[8–12]. Migratory functionalization via *cis*-1,2-palladium migration between sp^2 carbons has been rarely reported[13–19]. Another metal migration frequently exploited is a 1,4-metal shift in many transition metal-catalyzed tandem reactions[1,4,5].

Indenone and five-membered benzoheterocycles are ubiquitous structural motifs found in a wide array of natural products, pharmaceuticals, and agrochemicals (Fig. 2a)[20,21]. In particular, benzophosphole is widely used in developing functional materials[22–27], biologically active compounds[28–33], and chiral ligands[34–37]. The transition metal-catalyzed intramolecular coupling of aryl halides or aryl metals with alkenes has become a versatile tool in heterocycle synthesis (Fig. 2b, top)[38–43]. However, this traditional strategy requires the prior introduction of a halo or metal group at the *ortho* position of the aryl ring. Under this premise, we wondered whether an alternative synthetic route based on a cascade-type process involving 1,*n*-metal migration from an alkenyl carbon atom to an aryl carbon atom might be designed, thus setting the stage for carbometallation of a C=C double bond (Fig. 2b, bottom). Hayashi reported the Rh-catalyzed cyclization of arylpropargyl alcohols via a 1,4-Rh shift−aryl rhodation sequence, which validates our hypothesis[44–46]. The very wide availability of monosubstituted olefins ArX−CH=CH_2 and their facile conversion into ArX−CBr=CH_2 by simple bromination and elimination should make this new strategy very synthetically useful. At the outset of our investigations, however, it was unclear whether such a strategy could be implemented as elimination from ArX−CBr=CH_2 to give alkynes could be envisaged as being highly feasible.

Herein, we report the successful realization of this goal through a palladium-catalyzed migratory cyclization of α-bromoalkene derivatives ArXCBr=CH_2 **1**, in which the X moiety is a phosphine oxide, silyl, sulfonyl, carbonyl, amide, or oxygen atom/group, to give benzoheterocycles **2** (Fig. 2c). In this process, two C−H bonds are simultaneously cleaved and

[1]Inner Mongolia Key Laboratory of Low Carbon Catalysis, Inner Mongolia Key Laboratory of Synthesis and Application of Organic Functional Molecules, College of Chemistry and Chemical Engineering, Inner Mongolia University, Hohhot, China. [2]School of Chemistry and Chemical Engineering, Chongqing Key Laboratory of Chemical Theory and Mechanism, Chongqing University, Chongqing, China. [3]Natural Products Chem-Bio Innovation Center, College of Food and Bioengineering, College of Chemistry and Chemical Engineering, Chengdu University, Chengdu, China. [4]Inner Mongolia Academy of Science and Technology, Hohhot, China. [5]State Key Laboratory of Antiviral Drugs, Pingyuan Laboratory, Henan Normal University, Xinxiang, Henan, China. ✉e-mail: lanyu@cqu.edu.cn; shufengchen@imu.edu.cn; mingjialin@cdu.edu.cn

https://doi.org/10.1038/s41467-025-58633-5

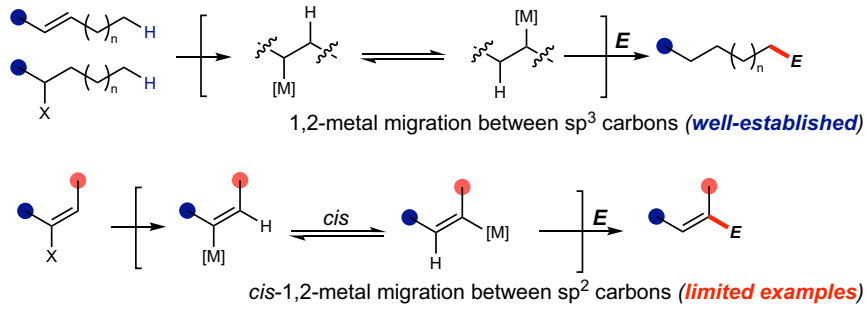

Fig. 1 | Migratory functionalization via 1,2-metal migration. 1,2-Metal migration between sp^3 or sp^2 carbons in catalytic cycles.

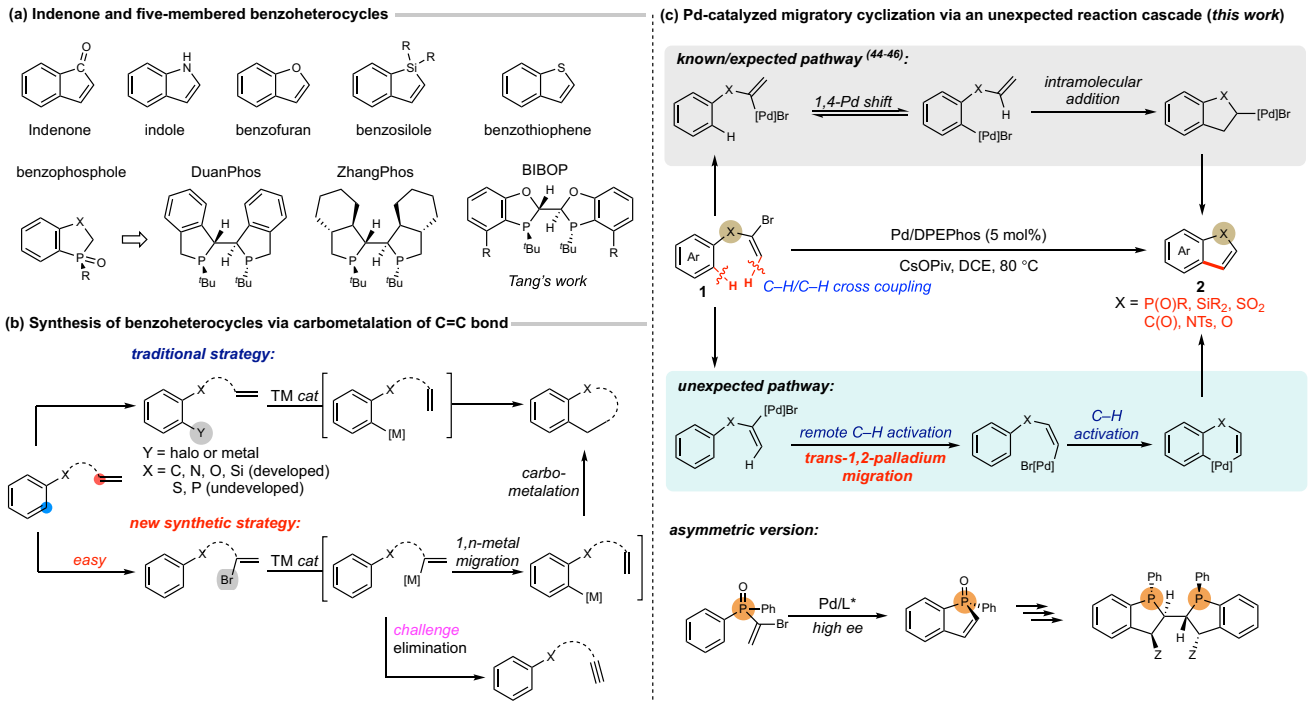

Fig. 2 | Transition metal-catalyzed migratory cyclization. a Indenone and five-membered benzoheterocycles. **b** Strategies to synthesize benzocycles. **c** This work: Pd-catalyzed migratory cyclization via an unexpected reaction cascade.

coupled to form a new carbon–carbon bond, whereas transition metal-catalyzed C–H/C–H coupling of arenes and alkenes always occurs via an aryl C–H metalation followed by a Heck-type alkenylation process[47–54]. However, the reaction does not proceed through an oxidative addition–1,4-palladium migration[55–61]–arylpalladation sequence as we expected. Detailed mechanistic studies have shown that *trans*-1,2-metal migration from the *α*-position to the *trans*-*β*-position of the C=C double bond is a key step of the catalytic cycle. This migratory cyclization is synthetically very useful and offers opportunities for the efficient synthesis of indoles and their phosphorus, silicon, sulfur, carbon, and oxygen congeners. Previously, 2,3-unsubstituted benzophosphole was prepared by ring-closing metathesis of phenylstyrylvinylphosphine oxide[62,63]. As reported herein, the present method enabled the efficient synthesis of benzophosphole oxides, and the asymmetric version of the cascade reaction was also achieved in the presence of a chiral palladium catalyst to give enantio-enriched P-chiral products.

Results

Optimization of the reaction conditions

In a first set of experiments, the cyclization of (*α*-bromoethenyl) diphenylphosphine oxide (**1a**) was performed in the presence of 5 mol % of palladium catalysts bearing several types of bisphosphine ligands and 2.0 equiv. of CsOPiv (OPiv = pivalate) in 1,2-dichloroethane (DCE) at 80 °C for 12 h (Table 1). The reaction with DPEPhos as a ligand gave a 94% yield of the cyclization product **2a** (entry 1). An alternative wide-bite-angle ligand, Xantphos, was not effective for the present reaction (entry 2). Some other bisphosphine ligands, such as dppf, dppe, dppp, dppb, and biphep, gave **2a** as the main product in somewhat lower yields (entries 3–7). The reaction performed in toluene afforded **2a** in moderate yield, whereas in CH_2Cl_2 it gave a mixture of **2a** and **2a'** in an 85:15 ratio (entries 8 and 9). The use of other bases, such as CsOAc and KOPiv, furnished **2a** in moderate yields with medium chemoselectivities (entries 10 and 11). The reaction performed at a lower temperature (60 °C) gave **2a** in a slightly lower yield (entry 12).

Pd-catalyzed migratory cyclization: substrate scope

Figure 3 summarizes the results obtained for the migratory cyclization of other $ArXCBr{=}CH_2$, in which X denotes phosphorus or another element, under the optimized conditions. Cyclizations of (*α*-bromoethenyl)diarylphosphine oxides **1b**–**1g**, in which the aromatic groups are phenyl moieties substituted with methyl, *t*-butyl, phenyl, methoxy, fluoro, and trifluoromethyl at the *para* position, proceeded well, giving the benzophospholes **2b**–**2g** in high yields, irrespective of the electronic properties of the substituents (Fig. 3). (*α*-

https://doi.org/10.1038/s41467-025-58633-5

Table 1 | Optimization of the reaction conditions

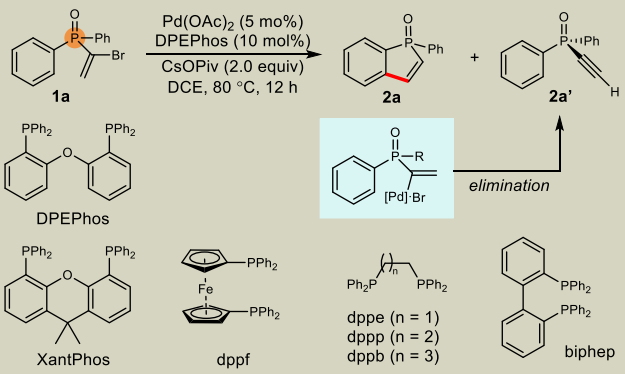

Entry	Variations from standard conditions[a] (shown above)	2a:2a'[b]	Yield (%)[c] 2a
1	None	>50:1	94
2	Xantphos	>50:1	41
3	Dppf	>50:1	82
4	Dppe	>50:1	46
5	Dppp	>50:1	13
6	Dppb	>50:1	23
7	Biphep	–	–
8	Toluene instead of DCE	>50:1	47
9	CH_2Cl_2 instead of DCE	85:15	78
10	CsOAc instead of CsOPiv	74:26	63
11	KOPiv instead of CsOPiv	89:11	72
12	At 60 °C	>50:1	87

[a] Reaction conditions: **1a** (0.20 mmol), $Pd(OAc)_2$ (5 mol% Pd), DPEPhos (10 mol%), CsOPiv (0.4 mmol), and DCE (1.0 mL) at 80 °C for 12 h.
[b] Ratio was determined by ^{1}H NMR analysis of the crude reaction mixture.
[c] Isolated yield.

Bromoethenyl)diarylphosphine oxides **1h**–**1k**, in which the aromatic groups are phenyl moieties substituted with methyl, methoxy, and trifluoromethyl at the *meta* position, all proved suitable for this reaction, affording exclusively the benzophospholes **2h**–**2k** in high yields, and the new C–C bonds were formed with high regioselectivity at the less hindered *ortho* C–H position. Moreover, *ortho*-substituted phenyl derivative **1l** gave 70% yield of the migratory cyclization product **2l**, the yield being lower due to some generation of the elimination by-product. The reaction of **1m**, bearing a benzo[*b*]thiophen-5-yl group, gave 67% yield of the corresponding product **2m** with high regioselectivity. The migratory cyclizations of alkyl-substituted (*α*-bromoethenyl)phenylphosphine oxides **1n**–**1r** also proceeded, furnishing the corresponding products **2n**–**2r** in moderate yields. The yields of **2n**–**2r** were moderate due to some generation of the elimination by-product.

The robustness of the present protocol was further demonstrated by the synthesis of other benzoheterocyclic compounds, in which the X moiety is an atom or group other than phosphine oxide (Fig. 3). It was found that the migratory cyclization of *α*-bromovinyl ketone **1s**, in which the X moiety of the substrate is a carbonyl group, was viable, giving the inden-1-one product **2s** in a high yield under the standard conditions. *N*-Tosylindoles **2t**–**2v**, in which X is a tosyl-protected amide group, were also efficiently obtained by using the present methodology. When the X moiety of the substrate was an oxygen atom, the migratory cyclization proceeded smoothly to afford benzofuran **2w** in 73% yield. Moreover, unsubstituted 1-silaindene **2x** was obtained in 63% yield under the present conditions. Benzo[*b*]thiophene 1-oxide and 1,1-dioxides are an emerging class of heterocyclic compounds with synthetic and medicinal chemistry applications[64–68]. Fortunately, the reaction of *α*-bromovinylphenyl sulfoxide **1y** gave the benzo[*b*]thiophene 1-oxide **2y** in 83% yield. The cyclizations of *α*-bromovinyl aryl sulfones **1z**–**1ab** also proceeded smoothly to afford benzo[*b*]thiophene 1,1-dioxides **2z**–**3ab** in high yields.

Asymmetric synthesis of P-chiral benzophospholes

To explore the potential of this methodology in asymmetric synthesis, a preliminary screening of chiral bisphosphine ligands was carried out. As shown in Fig. 4, reaction of **1a** in the presence of a chiral (*R*)-DM-segphos-palladium catalyst gave **2a** in 31% isolated yield with a promising 86% ee, whereby the relatively low yield was due to low conversion of **1a**. The asymmetric cyclization of (*α*-bromoethenyl) diarylphosphine oxide **1b**, in which the aromatic group is phenyl moiety substituted with methyl at the *para* position, gave the benzophosphole **2b** in 37% yield with 67% ee. The reaction of **1f**, bearing fluoro substitution at the *para* position of phenyl ring, gave the asymmetric cyclization product **2f** in 33% yield with 71% ee. The reaction of **1k**, bearing a 2-naphthyl group, gave 44% yield of the asymmetric cyclization product **2k** with 57% ee and high regioselectivity. The asymmetric cyclization of **1m**, bearing a benzo[*b*]thiophen-5-yl group, gave 29% yield of the corresponding product **2m** with 74% ee and high regioselectivity.

Mechanistic studies

Subsequently, we conducted preliminary experiments to provide insight into the reaction mechanism. We initially envisaged that the cyclization might proceed via an alkenyl-to-aryl 1,4-Pd migration as a key step. However, when the cyclization reaction of *α*-bromovinyl di(pentadeuteriophenyl)phosphine oxide (**1a**-d_{10}) was carried out under the standard conditions, the product was **2a**-d_9, bearing only nine deuterium atoms at the aryl carbon atoms (Fig. 5a, equation 1).

https://doi.org/10.1038/s41467-025-58633-5

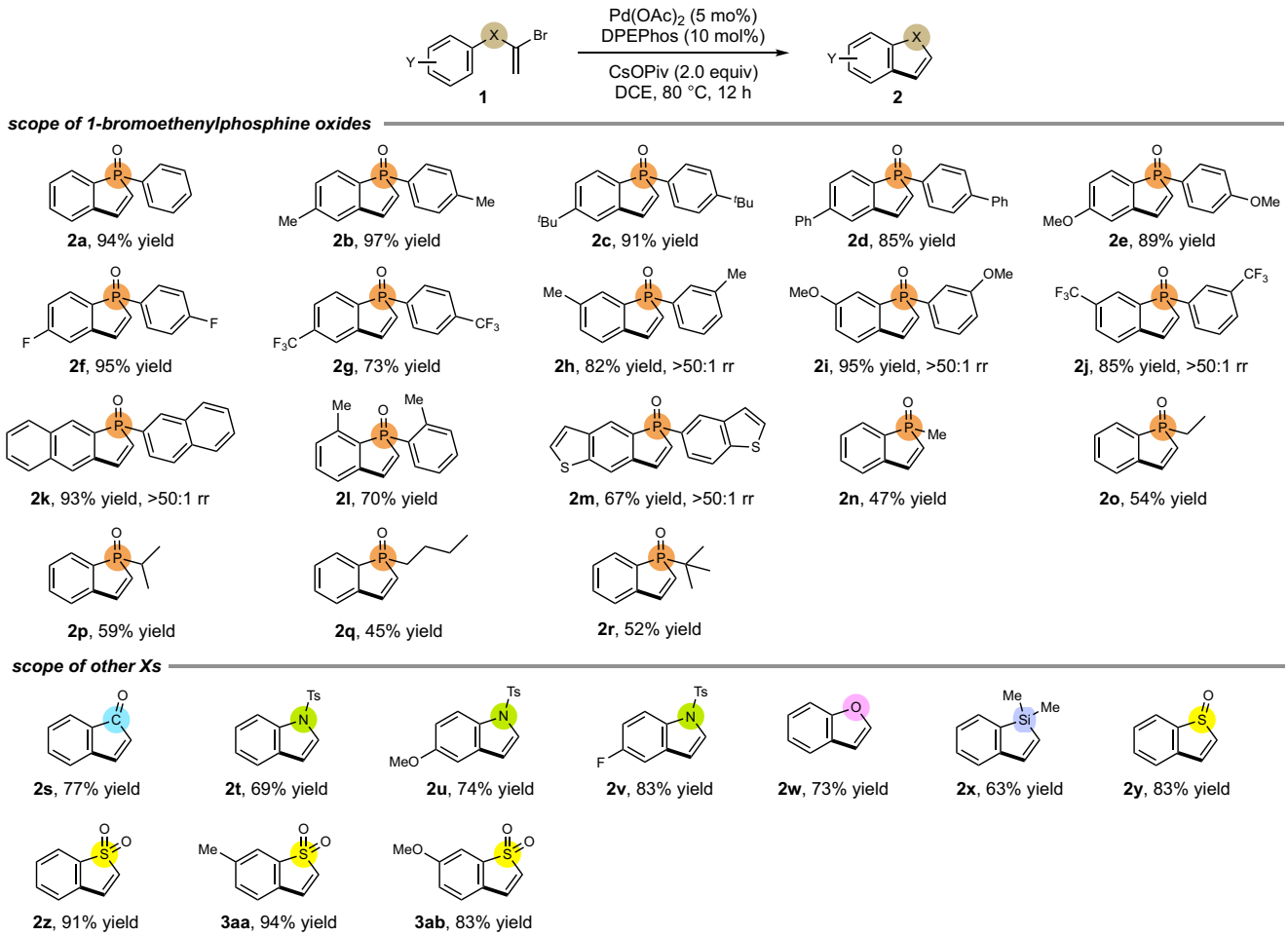

Fig. 3 | Pd-catalyzed migratory cyclization: substrate scope. Reaction conditions: **1** (0.20 mmol), $Pd(OAc)_2$ (5 mol% Pd), DPEPhos (10 mol%), CsOPiv (0.40 mmol), and DCE (1.0 mL) at 80 °C for 12 h. Isolated yield.

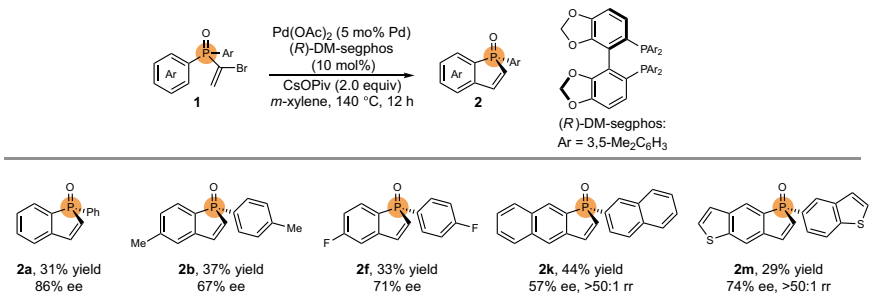

Fig. 4 | Asymmetric synthesis of P-chiral benzophospholes. Reaction conditions: **1** (0.20 mmol), $Pd(OAc)_2$ (5 mol% Pd), (*R*)-DM-segphos (10 mol%), CsOPiv (0.40 mmol), and *m*-xylene (1.0 mL) at 140 °C for 12 h. Isolated yield. The % ee was determined by HPLC on a chiral stationary phase column.

Furthermore, cyclization of *α*-bromovinyl di(2-deuteriophenyl)phosphine oxide (**1a**-d_2) under our standard conditions proceeded smoothly to give a mixture of **2a**-d_2 and **2a**-d_1 in a 2:1 ratio, with one or two deuterium atoms incorporated at the aryl carbon atoms (Fig. 5a, equation 2). No deuterium incorporation at the alkenyl carbon atoms of **2a**-d_9, **2a**-d_2, and **2a**-d_1 clearly demonstrated that no 1,4-palladium migration was involved in the catalytic cycle. The fact that reaction of **1z**-d_5 afforded benzothiophene sulfone **2z**-d_4 with no deuterium incorporated at the alkenyl carbon atoms further confirmed this conclusion (Fig. 5a, equation 3). Reaction of ethynyldiphenylphosphine oxide (**2a′**) in the presence of the DPEPhos-palladium catalyst, NEt_3·HBr, and CsOPiv gave the target product **2a** in 37% yield (Fig. 5b). As shown in Fig. 5c, cyclization of *Z*-(*β*-bromoethenyl)diphenylphosphine oxide (**3**) gave a 29% yield of **2a**. This indicated that the migratory cyclization might involve intramolecular C–H bond activation to form the C–C bond. Under the standard conditions, compound (*E*)-**4** afforded the elimination product **5** in high yield without formation of the cyclization product, whereas no reaction of its (*Z*)-isomer took place (Fig. 5d).

DFT calculations and proposed mechanism

Control experiments, in concert with DFT calculations[69–71](Fig. 6), were used to inform the development of a mechanistic model. The density functional theory (DFT) calculations at the M06L/6-311 + G(d,p)

https://doi.org/10.1038/s41467-025-58633-5

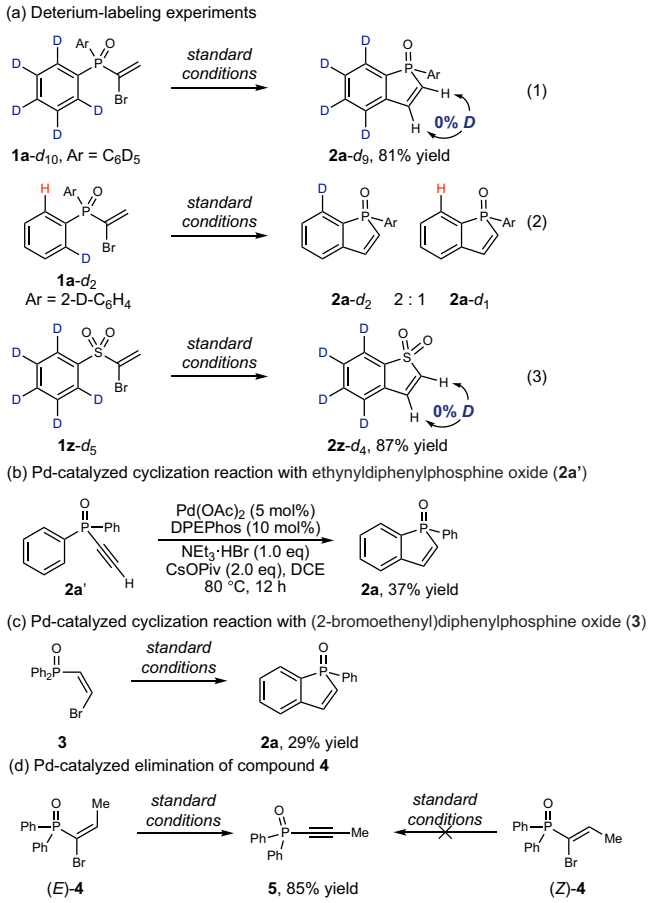

Fig. 5 | Mechanistic studies. a Deterium-labeling experiments. **b** Pd-catalyzed cyclization reaction with ethynyldiphenylphosphine oxide (**2a'**). **c** Pd-catalyzed cyclization reaction with (2-bromoethenyl)diphenylphosphine oxide (**3**). **d** Pd-catalyzed elimination of compound **4**.

(LANL2TZ for palladium atoms)/SMD(DCE)//B3LYP-D3/6-31G(d) (LANL2DZ for palladium atoms) level was performed to gain a theoretical understanding of the reaction mechanisms (see Supplementary Page S37). We chose the conversion of **1a** to **2a** as the model reaction, using $Pd(OAc)_2$ as the catalyst and DPEPhos as the ligand. Taking into account the coordination capability of olefins, the free energy profile is initiated by the Pd(0) species **INT-1**, wherein the ligand and the C=C bond are coordinated to the metal center. Subsequent C–Br bond oxidative addition to Pd center can occur via a three-membered ring-type transition state **2-ts** to form vinyl Pd(II) intermediate **INT-3** with an energy barrier of 22.9 kcal/mol, meanwhile releasing 7.5 kcal/mol of energy. In the presence of base, anion exchange of intermediate **INT-3** with $OPiv^-$ leads to the formation of the thermodynamically stable Pd(II)-OPiv intermediate **INT-4**. In the generated Pd(II)-OPiv intermediate **INT-4**, the Pd-OPiv and Pd-ethylene bond lengths are 2.11 and 2.03 Å, respectively, indicating weak Pd-O bonding. An outer-sphere deprotonation with the assistance of base then takes place to give the alkyne-coordinated Pd(II) intermediate **INT-6** via transition state **5-ts**, which is endergonic 5.0 kcal/mol. The energy barrier for this step is 23.7 kcal/mol. The Pd-C1 bond length and Pd-C2 bond length of Pd-ethylene in the transition state **5-ts** are 2.07 and 2.40 Å, respectively, which indicate that Pd center can activate the vinyl moiety. Sequential protonation occurs to form *cis*-vinyl Pd(II) intermediate **INT-8** via transition state **7-ts** with the energy barrier of 19.9 kcal/mol. The formed *cis*-vinyl Pd(II) intermediate **8** can easily isomerize to a *trans*-one **INT-9**[72,73]. The intramolecular phenylic C–H bond activation[74–79] of diphenylphosphine oxide happens through a concerted metalation-deprotonation (CMD) process via transition state **10-ts** to form a six-membered palladacycle **INT-11** with 1.4 kcal/mol exergonic, overcoming an energy barrier of 23.2 kcal/mol. Then a C–C bond reductive elimination generates the final product and regenerates Pd(0) species **INT-1** with an energy barrier of 12.7 kcal/mol. Meanwhile, we also explored the alternative blue and green pathways, which involves direct β-hydride elimination and phenylic C–H bond concerted metalation-deprotonation of intermediate **INT-4**. These pathways, however, have energy barrier of 27.5 and 44.1 kcal/mol, respectively, which are 3.8 kcal/mol and 20.4 kcal/mol higher than the pathway involving **5-ts**, indicating that these pathways are less favorable (see Supplementary Fig. 1).

According to the DFT calculations, we propose a plausible mechanism for the palladium-catalyzed migratory cyclization in Fig. 7. The mechanism involves C–Br oxidative addition of vinyl bromide, base-assisted outer-sphere deprotonation, sequential protonation, phenylic C–H bond concerted metalation-deprotonation and C–C bond reductive elimination. For comparative analysis, the direct β-hydride elimination pathway and the concerted metalation-deprotonation mechanism for the phenylic C–H bond are investigated using density functional theory; however, both pathways are determined to be energetically disfavored. The key *trans*−1,2-Pd migration core is driven by the cooperative C–H activation of the alkene coordinated to Pd. The electron-deficient Pd(II) center polarizes both the α- and β-carbons of the coordinated ethene, significantly weakening the terminal C–H bond. This electronic perturbation enables HOPiv to participate in an unconventional outer-sphere proton abstraction, bypassing the classical inner-sphere pathway. The resulting Pd–H intermediate undergoes stereochemical reversal migration and insertion, establishing a migration pathway distinct from the traditional β-hydride mechanism.

Synthesis of P-chiral bisphosphine ligands

Chiral bisphosphine ligands are of key importance in transition metal-catalyzed asymmetric synthesis of optically active products[34,37,80–83]. Enantio-enriched **2a** obtained above was reduced to 1-phenylphosphindane (R_P)-**6** in the presence of Pd/C and H_2 in 94% yield with >99.5% ee after recrystallization from methanol (Fig. 8a). Moreover, P-chiral bisphosphine ligand **L1** was easily prepared by treatment of (R_P)-**6** with the strong base lithium diisopropylamide and $CuCl_2$ in THF, followed by reduction with $HSiCl_3/NEt_3$ to give the product in an overall yield of 46%. Asymmetric addition of 4-$MeOC_6H_4B(OH)_2$ to **2a** in the presence of a chiral diene*-Rh catalyst proceeded smoothly to afford 3-arylated phosphindane (S_P,R_C)-**7** in 42% yield with >99.5% ee after recrystallization from methanol (Fig. 8b). Following the above steps, P-chiral bisphosphine ligand **L2** was also synthesized in an overall yield of 32%. **L1** and **L2** were then successfully directly used as chiral ligands in asymmetric hydrogenation to give compound **8** with 92% ee and 97% ee, respectively (Fig. 8c). The Hayashi–Miyaura reaction[84–91] of cyclohexanone and $PhB(OH)_2$ in the presence of the Rh/**L1** or Rh/**L2** catalysts also proceeded smoothly to give the 1,4-addition product **9** with >99% ee and 98% ee, respectively (Fig. 8d).

Discussion

In summary, we have reported a Pd-catalyzed migratory cyclization of $ArXCBr=CH_2$ to give In summary, we have reported a Pd-catalyzed migratory cyclization of $ArXCBr=CH_2$ to give benzoheterocycles, specifically indoles and their phosphorus, silicon, sulfur, carbon, and oxygen congeners. Detailed mechanistic studies have shown that the *trans*-1,2-palladium migration from the α-position to the *trans*-β-position of the C=C double bond is a key step of the catalytic cycle. The applicability of the present method has been showcased through the synthesis of new P-chiral bisphosphine ligands.

https://doi.org/10.1038/s41467-025-58633-5

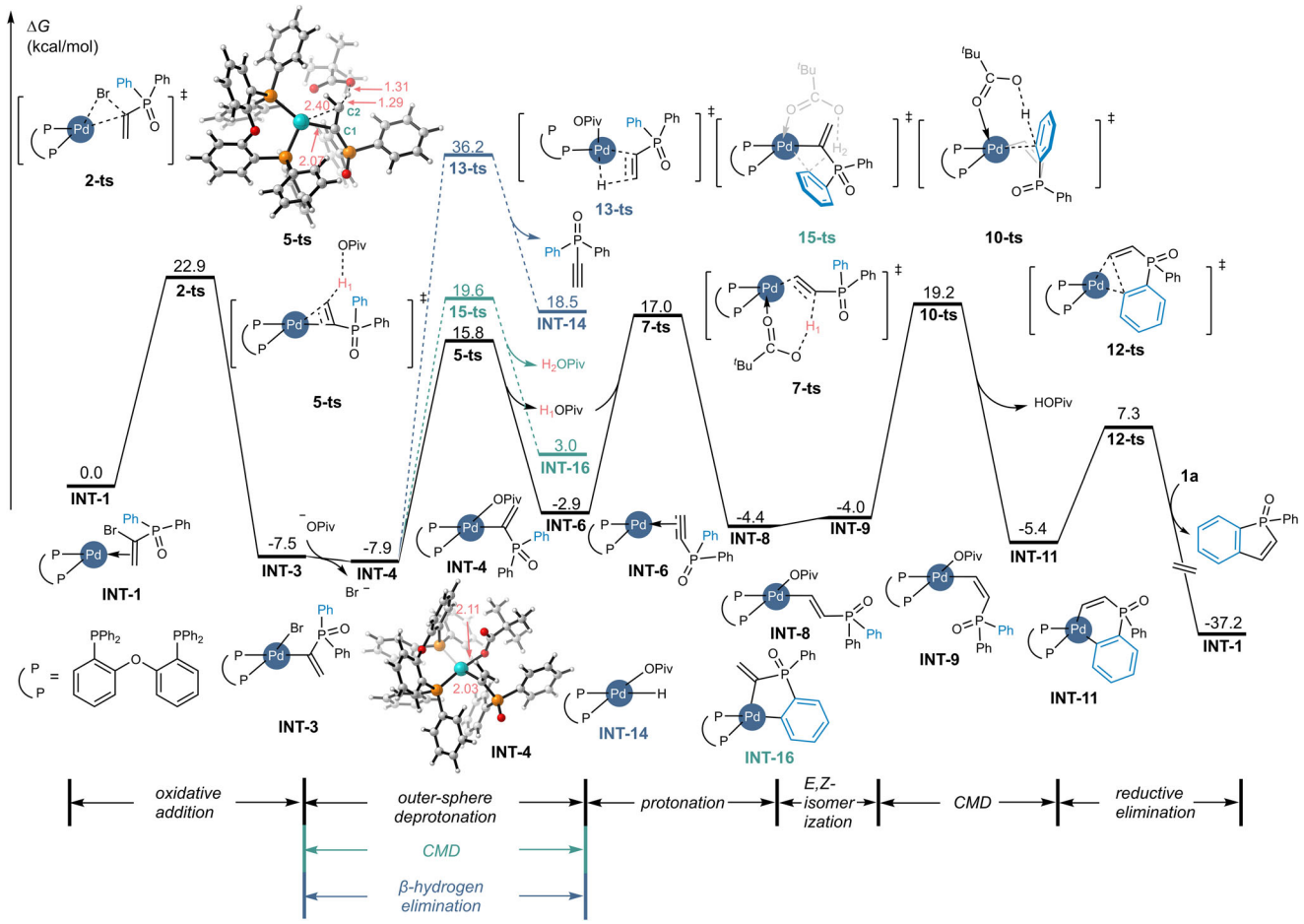

Fig. 6 | Free energy profile and selected transition state and intermediate structures for benzoheterocycles by palladium-catalyzed migratory cyclization. The energies are reported in kcal/mol and represent the relative free energies calculated using M06L/6-311 + G(d,p)(with LANL2TZ for palladium)/SMD(DCE)//B3LYP-D3/6-31G(d) (with LANL2DZ for palladium).

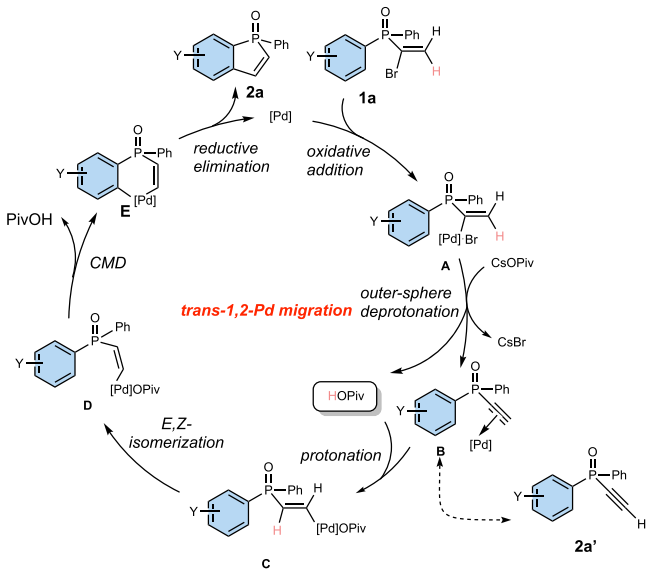

Fig. 7 | A proposed catalytic cycle for the palladium-catalyzed migratory cyclization of 1a. The catalytic cycle is proposed according to the control experiments and the DFT calculations.

Methods

A typical procedure for palladium-catalyzed migratory cyclization of ArXCBr=CH_2 (Table 1, entry 1)

An oven-dried sealed tube equipped with a PTFE-coated stir bar was charged with $Pd(OAc)_2$ (2.24 mg, 10 μmol, 5.0 mol% of Pd), **1a** (61.2 mg, 0.20 mmol), DPEPhos (10.8 mg, 20 μmol), CsOPiv (93.6 mg, 0.40 mmol) under argon. DCE (1.0 mL) was added successively, and the mixture was stirred at 80 °C for 12 h. The reaction mixture was passed through a short column of silica gel with dichloromethane as eluent and the water stayed in silica gel. The solvent was removed on a rotary evaporator. After ^{1}H NMR analysis of the residue, the crude product was subjected to silica gel chromatography (eluent:dichloromethane/methanol (30/1)) as the eluent to give **2a** (42.5 mg, 94% yield, 0.19 mmol) as a green solid.

A typical procedure for palladium-catalyzed asymmetric migratory cyclization of ArXCBr=CH_2 (Fig. 4)

An oven-dried sealed tube equipped with a PTFE-coated stir bar was charged with $Pd(OAc)_2$ (2.24 mg, 10 mmol, 5.0 mol% of Pd), **1a** (61.2 mg, 0.20 mmol), (*R*)-DM-segphos (14.5 mg, 20 mmol), CsOPiv (93.6 mg, 0.40 mmol) under argon. *m*-Xylene (1.0 mL) was added successively, and the mixture was stirred at 140 °C for 12 h. The reaction mixture was passed through a short column of silica gel with dichloromethane as eluent and the water stayed in silica gel. The solvent was removed on a rotary evaporator. After ^{1}H NMR analysis of the residue, the crude product was subjected to silica gel chromatography (eluent:dichloromethane/methanol (30/1)) as the eluent to give (*R*)-**2a** (14.0 mg, 31% yield, 0.062 mmol) as a green solid.

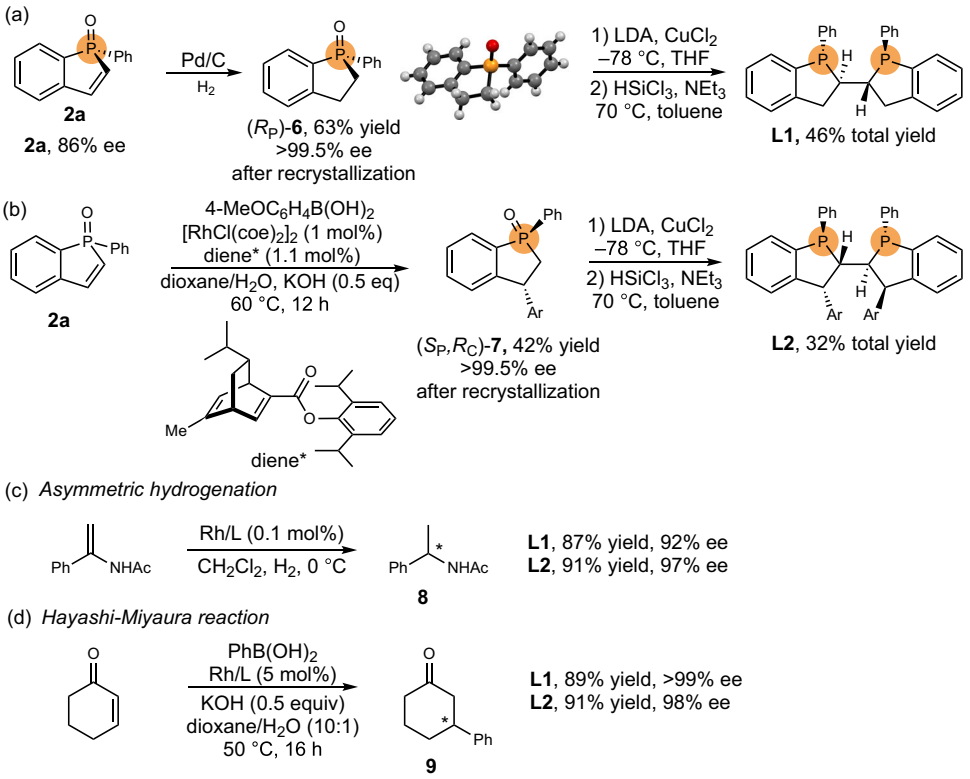

Fig. 8 | Synthesis of P-chiral bisphosphine ligands. a, **b** Asymmetric synthesis of P-chiral bisphosphine ligands. **c**, **d** Applications of these ligands in asymmetric synthesis.

Data availability

Detailed experimental procedures, characterization data, NMR spectra of new compounds, HPLC spectra for chiral compounds, detailed computational results, and calculated structures are available within Supplementary Information. Cartesian coordinates of the calculated structures are available from Source Data, which are provided with this paper. All the data supporting the findings of this work are available within the article and its Supplementary Information files or from the corresponding author upon request. Source data are provided with this paper.

References

1. Ma, S. & Gu, Z. 1,4-Migration of rhodium and palladium in catalytic organometallic reactions. *Angew. Chem. Int. Ed.* **44**, 7512–7517 (2005).
2. Shi, F. & Larock, R. C. Remote C–H activation via through-space palladium and rhodium migrations. *Top. Curr. Chem.* **292**, 123–164 (2010).
3. Croisant, M. F., Van Hoveln, R. & Schomaker, J. M. Formal dyotropic rearrangements in organometallic transformations. *Eur. J. Org. Chem.* **2015**, 5897–5907 (2015).
4. Rahim, A., Feng, J. & Gu, Z. 1,4-Migration of transition metals in organic synthesis. *Chin. J. Chem.* **37**, 929–945 (2019).
5. Li, M.-Y., Wei, D., Feng, C.-G. & Lin, G.-Q. Tandem reactions involving 1,4-palladium migrations. *Chem. Asian J.* **17**, e202200456 (2022).
6. Ju, C. W. & Zhao, D. Transition metal-catalyzed C–H bond functionalization involving metal migration. In *Handbook of CH-Functionalization*, 1–23 (Wiley, 2022).
7. Wang, Y., He, Y. & Zhu, S. Nickel-catalyzed migratory cross-coupling reactions: new opportunities for selective C–H functionalization. *Acc. Chem. Res.* **56**, 3475–3491 (2023).
8. Biswas, S. Mechanistic understanding of transition-metal-catalyzed olefin isomerization: metal-hydride insertion-elimination vs π-allyl pathways. *Comment. Inorg. Chem.* **35**, 301–331 (2015).
9. Vasseur, A., Bruffaerts, J. & Marek, I. Remote functionalization through alkene isomerization. *Nat. Chem.* **8**, 209–219 (2016).
10. Sommer, H., Juliá-Hernández, F., Martin, R. & Marek, I. Walking metals for remote functionalization. *ACS Cent. Sci.* **4**, 153–165 (2018).
11. Kochi, T., Kanno, S. & Kakiuchi, F. Nondissociative chain walking as a strategy in catalytic organic synthesis. *Tetrahedron Lett.* **60**, 150938 (2019).
12. Massad, I. & Marek, I. Alkene isomerization through allylmetals as a strategic tool in stereoselective synthesis. *ACS Catal.* **10**, 5793–5804 (2020).
13. Limmert, M. E., Roy, A. H. & Hartwig, J. F. Kumada coupling of aryl and vinyl tosylates under mild conditions. *J. Org. Chem.* **70**, 9364–9370 (2005).
14. Hansen, A. L. et al. Heck coupling with nonactivated alkenyl tosylates and phosphates: examples of effective 1,2-migrations of the alkenyl palladium(II) intermediates. *Angew. Chem. Int. Ed.* **45**, 3349–3353 (2006).
15. Ebran, J.-P., Hansen, A. L., Gøgsig, T. M. & Skrydstrup, T. Studies on the heck reaction with alkenyl phosphates: can the 1,2-migration be controlled? scope and limitations. *J. Am. Chem. Soc.* **129**, 6931–6942 (2007).
16. Watson, D. A. et al. Formation of ArF from LPdAr(F): catalytic conversion of aryl triflates to aryl fluorides. *Science* **325**, 1661–1664 (2009).
17. Lindhardt, A. T., Gøgsig, T. M. & Skrydstrup, T. Studies on the 1,2-migrations in Pd-catalyzed negishi couplings with josiPhos ligands. *J. Org. Chem.* **74**, 135–143 (2009).
18. Filatova, E. A., Gulevskaya, A. V., Pozharskii, A. F. & Ozeryanskii, V. A. Synthesis and some properties of alkynyl derivatives of 1,3-dialkylperimidones. An example of the 1,2-palladium migration in the Sonogashira reaction. *Tetrahedron* **72**, 1547–1557 (2016).
19. Sekiguchi, Y., Onnuch, P., Li, Y. & Liu, R. Migratory aryl cross-coupling. *J. Am. Chem. Soc.* **147**, 1224–1230 (2025).

20. Chowdhury, M. G. et al. A comprehensive account of synthesis and biological activities of α-lidene-benzocycloalkanones and benzo-heterocycles. *ChemistrySelect* **7**, e202201468 (2022).
21. Abbas, A. A., Farghaly, T. A. & Dawood, K. M. Recent advances on anticancer and antimicrobial activities of directly-fluorinated five-membered heterocycles and their benzo-fused systems. *RSC Adv.* **14**, 19752–19779 (2024).
22. Hissler, M., Dyer, P. W. & Réau, R. Linear organic π-conjugated systems featuring the heavy group 14 and 15 elements. *Coord. Chem. Rev.* **244**, 1–44 (2003).
23. Baumgartner, T. & Réau, R. Organophosphorus π-conjugated materials. *Chem. Rev.* **106**, 4681–4727 (2006).
24. Matano, Y. & Imahori, H. Design and synthesis of phosphole-based π systems for novel organic materials. *Org. Biomol. Chem.* **7**, 1258–1271 (2009).
25. Ren, Y. & Baumgartner, T. Combining form with function–the dawn of phosphole-based functional materials. *Dalton Trans.* **41**, 7792–7800 (2012).
26. Baumgartner, T. Insights on the design and electron-acceptor properties of conjugated organophosphorus materials. *Acc. Chem. Res.* **47**, 1613–1622 (2014).
27. Shameem, M. A. & Orthaber, A. Organophosphorus compounds in organic electronics. *Chem. Eur. J.* **22**, 10718–10735 (2016).
28. Allen, M. C. et al. Renin inhibitors. synthesis of transition-state analog inhibitors containing phosphorus acid derivatives at the scissile bond. *J. Med. Chem.* **32**, 1652–1661 (1989).
29. Smith, W. W. & Bartlett, P. A. Macrocyclic inhibitors of penicillopepsin. 3. design, synthesis, and evaluation of an inhibitor bridged between P2 and P1′. *J. Am. Chem. Soc.* **120**, 4622–4628 (1998).
30. Mucha, A., Kafarski, P. & Berlicki, Ł. Remarkable potential of the α-aminophosphonate/phosphinate structural motif in medicinal chemistry. *J. Med. Chem.* **54**, 5955–5980 (2011).
31. Clarion, L. et al. *C*-glycoside mimetics inhibit glioma stem cell proliferation, migration, and invasion. *J. Med. Chem.* **57**, 8293–8306 (2014).
32. Iwamoto, N. et al. Control of phosphorothioate stereochemistry substantially increases the efficacy of antisense oligonucleotides. *Nat. Biotechnol.* **35**, 845–851 (2017).
33. Knouse, K. W. et al. Unlocking P(V): reagents for chiral phosphorothioate synthesis. *Science* **361**, 1234–1238 (2018).
34. Tang, W. J. & Zhang, X. New chiral phosphorus ligands for enantioselective hydrogenation. *Chem. Rev.* **103**, 3029–3069 (2003).
35. Dutartre, M., Bayardon, J. & Jugé, S. Applications and stereoselective syntheses of P-chirogenic phosphorus compounds. *Chem. Soc. Rev.* **45**, 5771–5794 (2016).
36. Ni, H. Z., Chan, W.-L. & Lu, Y. X. Phosphine-catalyzed asymmetric organic reactions. *Chem. Rev.* **118**, 9344–9411 (2018).
37. Xu, G., Senanayake, C. H. & Tang, W. J. P-chiral phosphorus ligands based on a 2,3-dihydrobenzo[*d*][1,3]oxaphosphole motif for asymmetric catalysis. *Acc. Chem. Res.* **52**, 1101–1112 (2019).
38. Zeni, G. & Larock, R. C. Synthesis of heterocycles via palladium-catalyzed oxidative addition. *Chem. Rev.* **106**, 4644–4680 (2006).
39. Platon, M., Amardeil, R., Djakovitch, L. & Hierso, J.-C. Progress in palladium-based catalytic systems for the sustainable synthesis of annulated heterocycles: a focus on indole backbones. *Chem. Soc. Rev.* **41**, 3929–3968 (2012).
40. Wu, X.-F., Neumann, H. & Beller, M. Synthesis of heterocycles via palladium-catalyzed carbonylations. *Chem. Rev.* **113**, 1–35 (2013).
41. Kaur, N. Palladium-catalyzed approach to the synthesis of *S*-heterocycles. *Catal. Rev.* **57**, 478–564 (2015).
42. Kaur, N. Palladium catalysts: synthesis of five-membered *N*-heterocycles fused with other heterocycles. *Catal. Rev.* **57**, 1–78 (2015).
43. Braun, M. Stereoselective domino heck-suzuki reactions. *Eur. J. Org. Chem.* **26**, e202201282 (2023).
44. Shintani, R., Okamoto, K. & Hayashi, T. Rhodium-catalyzed isomerization of α-arylpropargyl alcohols to indanones: involvement of an unexpected reaction cascade. *J. Am. Chem. Soc.* **127**, 2872–2873 (2005).
45. Shintani, R. & Hayashi, T. Rhodium-catalyzed addition of arylzinc reagents to aryl alkynyl ketones: synthesis of *β*,*β*-disubstituted indanones. *Org. Lett.* **7**, 2071–2073 (2005).
46. Shintani, R. et al. Rhodium-catalyzed asymmetric synthesis of indanones: development of a new "axially chiral" bisphosphine ligand. *J. Am. Chem. Soc.* **128**, 2772–2773 (2006).
47. Alberico, D., Scott, M. E. & Lautens, M. Aryl–aryl bond formation by transition-metal-catalyzed direct arylation. *Chem. Rev.* **107**, 174–238 (2007).
48. Liu, C., Zhang, H., Shi, W. & Lei, A. Bond formations between two nucleophiles: transition metal catalyzed oxidative cross-coupling reactions. *Chem. Rev.* **111**, 1780–1824 (2011).
49. Le Bras, J. & Muzart, J. Intermolecular dehydrogenative heck reactions. *Chem. Rev.* **111**, 1170–1214 (2011).
50. Yeung, C. S. & Dong, V. M. Catalytic dehydrogenative cross-coupling: forming carbon–carbon bonds by oxidizing two carbon –hydrogen bonds. *Chem. Rev.* **111**, 1215–1292 (2011).
51. Liu, C. et al. Oxidative coupling between two hydrocarbons: an update of recent C–H functionalizations. *Chem. Rev.* **115**, 12138–12204 (2015).
52. Yang, Y., Lan, J. & You, J. Oxidative C–H/C–H coupling reactions between two (hetero)arenes. *Chem. Rev.* **117**, 8787–8863 (2017).
53. Gandeepan, P. et al. 3d transition metals for C–H activation. *Chem. Rev.* **119**, 2192–2452 (2019).
54. Liang, Y.-F. et al. Carbon–carbon bond cleavage for late-stage functionalization. *Chem. Rev.* **123**, 12313–12370 (2023).
55. Zhao, J. & Larock, R. C. Synthesis of substituted carbazoles, indoles, and dibenzofurans by vinylic to aryl palladium migration. *J. Org. Chem.* **71**, 5340–5348 (2006).
56. Hu, T.-J. et al. Highly stereoselective synthesis of 1,3-dienes through an aryl to vinyl 1,4-palladium migration/heck sequence. *Angew. Chem. Int. Ed.* **57**, 5871–5875 (2018).
57. Wei, D., Hu, T.-J., Feng, C.-G. & Lin, G.-Q. Synthesis of substituted naphthalenes by 1,4-palladium migration involved annulation with internal alkynes. *Chin. J. Chem.* **36**, 743–748 (2018).
58. Lin, J. et al. Tunable construction of multisubstituted 1,3-dienes and allenes via a 1,4-palladium migration/carbene insertion cascade. *J. Org. Chem.* **87**, 12019–12035 (2022).
59. Chen, Y.-Z. et al. Highly stereoselective synthesis of 2,2-disubstituted vinylphosphonates via aryl to vinyl 1,4-palladium migration. *Chin. J. Chem.* **40**, 2188–2192 (2022).
60. Chen, Z.-Y. et al. Highly stereoselective synthesis of 1,3-enynes via aryl to vinyl 1,4-palladium migration/sonogashira coupling sequence. *ChemCatChem* **16**, e202400478 (2024).
61. Tsitopoulou, M., Clemenceau, A., Thesmar, P. & Baudoin, O. 1,4-Pd migration-enabled synthesis of fused 4-membered rings. *J. Am. Chem. Soc.* **146**, 18811–18816 (2024).
62. Matsuda, T., Yamaguchi, Y. & Murakami, M. Synthesis of silole skeletons via metathesis reactions. *Synlett* **2008**, 561–564 (2008).
63. Carr, D. J. et al. Synthesis of 2,3-dihydro-1-phenylbenzo[*b*]phosphole (1-Phenylphosphindane) and its use as a mechanistic test in the asymmetric appel reaction: decisive evidence against involvement of pseudorotation in the stereoselecting step. *J. Org. Chem.* **78**, 10500–10505 (2013).
64. Mansuy, D. et al. Thiophene S-oxides as new reactive metabolites: formation by cytochrome P-450 dependent oxidation and reaction with nucleophiles. *J. Am. Chem. Soc.* **113**, 7825–7826 (1991).
65. Villar, R. et al. Synthesis and cytotoxic activity of lipophilic sulphonamide derivatives of the benzo[*b*]thiophene 1,1-dioxide. *Bioorg. Med. Chem.* **12**, 963–968 (2004).

66. Encío, I. et al. Benzo[*b*]thiophenesulphonamide 1,1-dioxide derivatives inhibit tNOX activity in a redox state-dependent manner. *Br. J. Cancer* **92**, 690–695 (2005).
67. Chandrasekera, N. S. et al. Synthesis and *anti*-tubercular activity of 3-substituted benzo[*b*]thiophene-1,1-dioxides. *Peerj* **2**, e612 (2014).
68. Kummari, L. K. et al. Antifungal benzo[*b*]thiophene 1,1-dioxide IMPDH inhibitors exhibit pan-assay interference (PAINS) profiles. *Bioorg. Med. Chem.* **26**, 5408–5419 (2018).
69. Qi, X. & Lan, Y. Recent advances in theoretical studies on transition-metal-catalyzed carbene transformations. *Acc. Chem. Res.* **54**, 2905–2915 (2021).
70. He, X., Zhong, K., Heng, D. & Zeng, Z. Is the metal involved or not? A computational study of Cu(I)-catalyzed [4 + 1] annulation of vinyl indole and carbene precursor. *Chin. Chem. Lett.* **33**, 2031–2035 (2022).
71. Zhong, K., Liu, S., He, X.& Ni, H. Oxidative cyclopalladation triggers the hydroalkylation of alkynes. *Chin. Chem. Lett.* **34**, 108339 (2023).
72. Lv, W. et al. Palladium-catalyzed intermolecular *trans*-selective carbofunctionalization of internal alkynes to highly functionalized alkenes. *ACS Catal.* **10**, 10516–10522 (2020).
73. Shan, C. et al. Mechanistic insight into *anti*-carbometalation of an alkyne *via* η^2-vinyl-nickel type *Z*/*E* isomerization. *Org. Chem. Front.* **10**, 4243–4249 (2023).
74. Chen, X., Engle, K. M., Wang, D. H. & Yu, J. Q. Palladium(II)-catalyzed C–H activation/C–C cross-coupling reactions: versatility and practicality. *Angew. Chem. Int. Ed.* **48**, 5094–5115 (2009).
75. Lyons, T. W. & Sanford, M. S. Palladium-catalyzed ligand-directed C –H functionalization reactions. *Chem. Rev.* **110**, 1147–1169 (2010).
76. Davies, H. M. L., Du Bois, J. & Yu, J.-Q. C–H functionalization in organic synthesis. *Chem. Soc. Rev.* **40**, 1855–1856 (2011).
77. Engle, K. M., Mei, T.-S., Wasa, M. & Yu, J.-Q. Weak coordination as a powerful means for developing broadly useful C–H functionalization reactions. *Acc. Chem. Res.* **45**, 788–802 (2012).
78. Diesel, J. & Cramer, N. Generation of heteroatom stereocenters by enantioselective C–H functionalization. *ACS Catal.* **9**, 9164–9177 (2019).
79. Shao, Q. et al. From $Pd(OAc)_2$ to chiral catalysts: the discovery and development of bifunctional mono-N-protected amino acid ligands for diverse C–H functionalization reactions. *Acc. Chem. Res.* **53**, 833–851 (2020).
80. Zhang, W., Chi, Y. & Zhang, X. Developing chiral ligands for asymmetric hydrogenation. *Acc. Chem. Res.* **40**, 1278–1290 (2007).
81. Zhao, Q. et al. Noncovalent interaction-assisted ferrocenyl phosphine ligands in asymmetric catalysis. *Acc. Chem. Res.* **53**, 1905–1921 (2020).
82. Wan, F. & Tang, W. J. Phosphorus ligands from the zhang lab: design, asymmetric hydrogenation, and industrial applications. *Chin. J. Chem.* **39**, 954–968 (2021).
83. Cao, Z., He, D. Y. & Tang, W. J. Catalysis and synthesis enabled by P-chiral dihydrobenzooxaphosphole ligands. *Org. Process. Res. Dev.* **28**, 949–977 (2024).
84. Hayashi, T. & Yamasaki, K. Rhodium-catalyzed asymmetric 1,4-addition and its related asymmetric reactions. *Chem. Rev.* **103**, 2829–2844 (2003).
85. Tian, P., Dong, H.-Q. & Lin, G.-Q. Rhodium-catalyzed asymmetric arylation. *ACS Catal.* **2**, 95–119 (2011).
86. Jean, M., Casanova, B., Gnoatto, S. & van de Weghe, P. Strategy of total synthesis based on the use of Rh-catalyzed stereoselective 1,4-addition. *Org. Biomol. Chem.* **13**, 9168–9175 (2015).
87. Heravi, M. M., Dehghani, M. & Zadsirjan, V. Rh-catalyzed asymmetric 1,4-addition reactions to *α*,*β*-unsaturated carbonyl and related compounds: an update. *Tetrahedron.: Asymmetry* **27**, 513–588 (2016).
88. Burns, A. R., Lam, H. W. & Roy, I. D. Enantioselective, rhodium-catalyzed 1,4-addition of organoboron reagents to electron-deficient alkenes. *Org. React.* **93**, 1–686 (2017).
89. Huang, Y. & Hayashi, T. Chiral diene ligands in asymmetric catalysis. *Chem. Rev.* **122**, 14346–14404 (2022).
90. Yin, L. et al. Asymmetric synthesis of P-stereogenic phosphindane oxides via kinetic resolution and their biological activity. *Nat. Commun.* **15**, 2548 (2024).
91. Li, W.-C., Ming, J. & Chen, S. Kinetic resolution of P-chiral phosphindole oxides through rhodium-catalyzed asymmetric arylation. *Org. Lett.* **26**, 3987–3990 (2024).

Acknowledgements

This work was supported by the National Natural Science Foundation of China (22261039, 22461028, and 21901132), the Program for Innovative Research Team in Universities of Inner Mongolia Autonomous Region (NMGIRT2324), the Science and Technology Leading Talent Team in Inner Mongolia Autonomous Region (2022LJRC0001), and the Inner Mongolia Institute of Science and Technology Industrial Technology Innovation Program (2024RCYJ02005). We also acknowledge the support from Center of Advanced Analysis & Gene Sequencing of Zhengzhou University.

Author contributions

J.M. conceived the idea and guided the project. W.L., J.Z., S.B., and G.L. performed the experiments and analyzed the data. Y.L. directed the part of computational study. L.Z. carried out the computational study. J.M. and S.C. wrote the manuscript. All authors approved the submission of the manuscript.

Competing interests

The authors declare no competing interests.

Additional information

Supplementary information The online version contains supplementary material available at https://doi.org/10.1038/s41467-025-58633-5.

Correspondence and requests for materials should be addressed to Yu Lan, Shufeng Chen or Jialin Ming.

Peer review information *Nature Communications* thanks the anonymous reviewers for their contribution to the peer review of this work. A peer review file is available.